Chapter 4: Evaluation of the antioxidant capacity of the *Hemidesmus indicus* and *Ichnocarpus frutescens* extracts and their phytoconstituents

4.1 Introduction

During regular metabolic activities, the human body produces a range of reactive oxygen species (ROS), including hydrogen peroxide, superoxide anions, and hydroxyl ions. These ROS, while necessary for certain cellular functions, can cause oxidative stress when present in excess, leading to damage to cells and tissues. Numerous chronic diseases, such as diabetes, cancer, and cardiovascular ailments, are linked to oxidative stress (Ozougwu, 2016; Sharifi-Rad et al., 2020).

To counteract the detrimental effects caused by ROS, the body relies on a defence system composed of antioxidant enzymes and non-enzymatic antioxidants. Major antioxidant enzymes comprise glutathione peroxidase, which lowers lipid peroxides and hydrogen peroxide, catalase, which turns hydrogen peroxide into water and oxygen, and superoxide dismutase (SOD), that catalyzes the dismutation of superoxide radicals into oxygen and hydrogen peroxide. In addition to these enzymes, non-enzymatic antioxidants like vitamins C and E, as well as various phytochemicals like phenolics and flavonoids, play crucial roles in neutralizing ROS (Sindhi et al., 2013).

Xanthine oxidase is an enzyme that contributes to ROS production by generating superoxide anions during the oxidation of hypoxanthine to xanthine and subsequently from xanthine to uric acid (Borges et al., 2002; Liu et al., 2021). Because of its role in producing superoxide anions, inhibiting xanthine oxidase is a promising strategy to reduce oxidative stress and mitigate cellular damage (Malik et al., 2018). Therefore, in this chapter, xanthine oxidase was selected as a target enzyme to evaluate the antioxidant

potential of phytoconstituents silychristin and hyperoside isolated from *Hemidesmus indicus* and *Ichnocarpus frutescens*.

Additional assays were employed to further explore the antioxidant capacity of these phytoconstituents and root extract of *Hemidesmus indicus* and *Ichnocarpus frutescens*. The DPPH (2,2-diphenyl-1-picrylhydrazyl) assay is a commonly used method for assessing the free radical scavenging ability of compounds (Xie and Schaich, 2014). DPPH is a stable free radical characterized by its deep purple colour, which absorbs at 517 nm (Baliyan et al., 2022). When DPPH encounters an antioxidant, it gains a hydrogen atom and is reduced to DPPH-H, resulting in a colour change from purple to yellow. The extent of this colour change is proportional to the antioxidant capacity of the test compound (Flieger et al., 2021).

Ferric Reducing Antioxidant Power (FRAP) is another assay employed in this chapter. It assesses how well antioxidants can convert ferric ions (Fe3+) to ferrous ions (Fe2+) (Benzie and Devaki, 2018). In this assay, ferric ion forms a complex with 2,4,6-tripyridyl-s-triazine (TPTZ), which is colourless. Upon reduction by an antioxidant, the complex changes to a blue-coloured ferrous-TPTZ complex, indicating the antioxidant capacity of the sample (Ghoora et al., 2020; Hayes et al., 2011).

By employing a combination of computational studies on xanthine oxidase inhibition and experimental assays such as DPPH and FRAP, This chapter intends to offer an extensive evaluation of the antioxidant potential of root extract of *Hemidesmus indicus* and *Ichnocarpus frutescens* and their isolated compound silychristin and hyperoside. These findings will contribute to our understanding of how these bioactive compounds can mitigate oxidative stress and offer therapeutic benefits.

4.2 Materials and Methods

4.2.1 DPPH Free Radical Scavenging Assay

The antioxidant potential of the plant extracts and phytoconstituents was evaluated using the DPPH (2,2-diphenyl-1-picrylhydrazyl) free radical scavenging assay, utilizing the process described by Hsouna et al., with minor changes (Hsouna et al., 2011). To prepare for the assay, a 0.1 mM solution of DPPH was made and Various concentrations of the plant extracts and phytoconstituents were prepared, ranging from 5 µg/mL to 30 µg/mL, by diluting the stock solution of each extract with methanol. A well-known antioxidant, L-ascorbic acid served as a positive control., and it was also tested at similar concentrations. For each concentration, 3 mL of the sample was mixed with 1 mL of the DPPH solution in a test tube. Methanol solvent was used as the negative control. All the mixtures were incubated for half an hour at room temperature in the dark. The dark conditions were maintained to prevent the degradation of DPPH, which is sensitive to light. Using a spectrophotometer, the absorbance was determined at 517 nm. Using the following formula, the scavenging activity was calculated as:

$$\boldsymbol{Inhibition\ Percentage} = [(\boldsymbol{Ac - As}) \div \mathrm{Ac}] \times 100$$

where Ac is the absorbance of the control, and As is the absorbance of the sample.

4.2.2 Ferric Reducing Antioxidant Power (FRAP) Assay

The FRAP assay was carried out employing the method given by Wei et al., with minor changes (Wei et al., 2023). The FRAP reagent was prepared by mixing 10 mmol/L TPTZ solution, 20 mmol/L $FeCl_3 \cdot 6H_2O$ solution, and 0.3 mol/L acetate buffer at pH 3.6. The TPTZ reagent is a chromogenic agent, which forms a colorless complex with ferric ions. When the ferric ion (Fe^{3+}) in this complex is reduced to the ferrous form (Fe^{2+}) by an antioxidant, an intense blue color is produced, which can be quantified spectrophotometrically. To perform the assay, 900 µL of the freshly prepared FRAP

reagent was mixed with 70 µL of Milli-Q water and 30 µL of the samples at varying concentrations (20–120 µL). Milli-Q water was used as the negative control. The reaction mixture was incubated at 37°C for 30 minutes to allow for complete reduction of the ferric-TPTZ complex. A spectrophotometer was used to detect the absorbance at 593 nm, and the following formula was used to determine the antioxidant activity:

$$\boldsymbol{Inhibition\ Percentage} = [(\boldsymbol{Ac} - \boldsymbol{As}) \div \mathrm{Ac}] \times 100$$

where Ac is the absorbance of the control, and As is the absorbance of the sample.

4.2.3 Drug-Likeness and ADMET Profiling

The automated SwissADMET online server was utilized to measure the drug-likeness and pharmacokinetic properties of hyperoside and silychristin bioactive phytochemicals (Daina et al., 2017; Van De Waterbeemd and Gifford, 2003). Based on a drug's capacity to satisfy the requirements of absorption, distribution, metabolism, excretion, and toxicity, its effectiveness is anticipated. This is done by applying Lipinski's rule of five to evaluate a number of attributes, including molecular weight, number of rotatable bonds, hydrogen bond donors, hydrogen bond acceptors, bioavailability score, molar refractivity, and solubility. (Lipinski, 2004). AMES toxicity and skin toxicity test of the ligands were evaluated using Biovia Discovery Studio and pkCSM online server (Biovia, 2017; Pires et al., 2015)

4.2.4 Computational Study

4.2.4.1 Retrieval and Processing of Ligands

The phytochemicals hyperoside and silychristin isolated from *Ichnocarpus frutescens* and *Hemidesmus indicus* were selected to study their antioxidant potential compared to Ascorbic Acid as a positive control through a molecular docking study. Because ascorbic acid has a well-established antioxidant potential and is known to have inhibitory activity against xanthine oxidase (Ho et al., 2021; Saftić Martinović et al., 2023). Ascorbic acid

is widely recognized in both experimental and computational research as a standard comparator for evaluating antioxidant properties. Its inclusion in the in silico analysis provided a meaningful benchmark for assessing the binding affinity and molecular interactions of the bioactive phytochemicals derived from the test samples.

The 3D structures of these ligands were retrieved from the NCBI PubChem database https://pubchem.ncbi.nlm.nih.gov (Kim, 2021, 2016) in SDF (Spatial Data File). The ligands were converted into. mae format using the LigPrep module in the Schrödinger suite (Schrödinger, LLC, New York, USA, 2022) (Olawale et al., 2022). During the ligand preparation, the OPLS4 (Optimized Potentials for Liquid Simulations) force field was applied, and the ionization states were generated at pH 7.0 ± 2.0, ensuring appropriate protonation under physiological conditions. Each ligand was prepared to generate a single isomer and automatic ion neutralization was performed (Madhavi Sastry et al., 2013). This process ensured that the ligands were in their optimal 3D conformations, suitable for subsequent molecular docking and dynamics simulations

4.2.4.2 Retrieval and Processing of Target Protein

The target protein for this study was Xanthine Oxidase, a crucial enzyme involved in purine metabolism and a target for inhibiting hyperuricemia and gout. The 3D crystal structure of Xanthine Oxidase was downloaded from the RCSB Protein Data Bank http://www.rcsb.org (Burley et al., 2019) with the PDB ID 3NVY (Zhang et al., 2021)

The protein structure was prepared using the Protein Preparation Wizard in Schrödinger, which involved adding hydrogens, assigning correct bond orders, and optimizing the structure. Water molecules that were not involved in key ligand interactions were removed, and energy minimization was performed using the OPLS4 force field to eliminate any steric clashes and optimize the geometry (Madhavi Sastry et al., 2013;

Shelley et al., 2007). After preparation, the Receptor Grid Generation tool in Glide was used to define the active site, centered on the co-crystallized ligand, with van der Waals scaling set to 1.0 and partial charge cutoff set to 0.25. This prepared grid was used for subsequent molecular docking simulations (Iwaloye et al., 2020).

4.2.4.3 Molecular Docking Simulations

Molecular docking was conducted through the Glide module in Schrödinger (Rajagopal et al., 2021) to analyze the binding interactions between Xanthine Oxidase and the ligands Silychristin, Hyperoside, and Ascorbic Acid. First, the docking protocol was validated by re-docking the co-crystallized ligand into the Xanthine Oxidase active site, ensuring that the Root Mean Square Deviation (RMSD) between the native and re-docked poses was ≤ 2.0 Å (Lolok et al., 2022). Following this validation, the three ligands were docked using the Standard Precision (SP) docking protocol, generating 10 docking poses for each ligand (Cross et al., 2009). Post-docking minimization was applied to further refine the ligand poses. The docking results were evaluated based on the GlideScore (docking score), the binding energy, and the specific interactions between the ligands and key residues within the active site of Xanthine Oxidase. The best docking poses were selected based on their binding affinities and interaction profiles for further analysis through molecular dynamics simulations.

4.2.4.4 Molecular Dynamics (MD) Simulations

The stability of complexes was further assessed through MD simulations through the Schrödinger Suite's Desmond simulation tool. The TIP3P system was used to solvate the orthorhombic box, and the OPLS4 force field was used to increase the solvent buffer by 10 Å around the protein. (Lu et al., 2021). After that, the system was neutralized and kept at a salt concentration of 0.15M by adding the requisite NaCl counter ions.

The system was equilibrated using Desmond's standard six-stage relaxation protocol under the constant NVT environment over 100 ps at the temperature of 10 K. Then equilibration was conducted under the constant NPT environment where the temperature was progressively raised to 310 K over 10 ps at a pressure of 1 bar. After that, production MD simulation was conducted for 200 ns at 310 K and 1 bar, and trajectories were recorded at 0.1 ns intervals for analysis.

The binding free energy (ΔG_{bind}) was determined by analyzing the last 10 ns of each MD trajectory employing Schrödinger's Prime MM/GBSA (Molecular Mechanics/Generalized Born Surface Area) technique (Azam et al., 2021). The following equation has been utilized to determine the binding free energy:

$$\Delta G_{bind} = \Delta G_{complex} - [\Delta G_{protein} + \Delta G_{ligand}]$$

where ΔG_{bind} represents the free energy of binding, $\Delta G_{protein}$ is the binding energy of the Xanthine Oxidase enzyme, and ΔG_{ligand} is the binding energy of the respective ligands (Silychristin, Hyperoside, and Ascorbic Acid) (Owoloye et al., 2022; Shao et al., 2023; Zhong et al., 2020).

4.3 Results and Discussions

4.3.1 DPPH Assay

The DPPH assay was utilized to evaluate the free radical scavenging activity of antioxidants, reflecting their ability to donate hydrogen atoms or electrons to neutralize free radicals. In this, the inhibition percentage of DPPH radicals was measured at various concentrations (5–30 µg/mL) for different phytochemicals, including Hyperoside, Silychristin, and methanolic extract of *Hemidesmus indicus* (H.I.), and *Ichnocarpus frutescens* (I.F.) and standard drug Ascorbic Acid. DPPH free radical scavenging activity of different concentrations of phytochemicals, extracts of *Hemidesmus indicus* and

Ichnocarpus frutescens, and the standard drug, Ascorbic Acid, has been illustrated in Figure 4.1. Ascorbic acid, a well-known antioxidant, demonstrates significant free radical scavenging activity, achieving inhibition rates close to 90% at higher concentrations (25 and 30 µg/mL). This high level of inhibition highlights its potent antioxidant capability, with an IC_{50} value of 15.75 µg/mL.

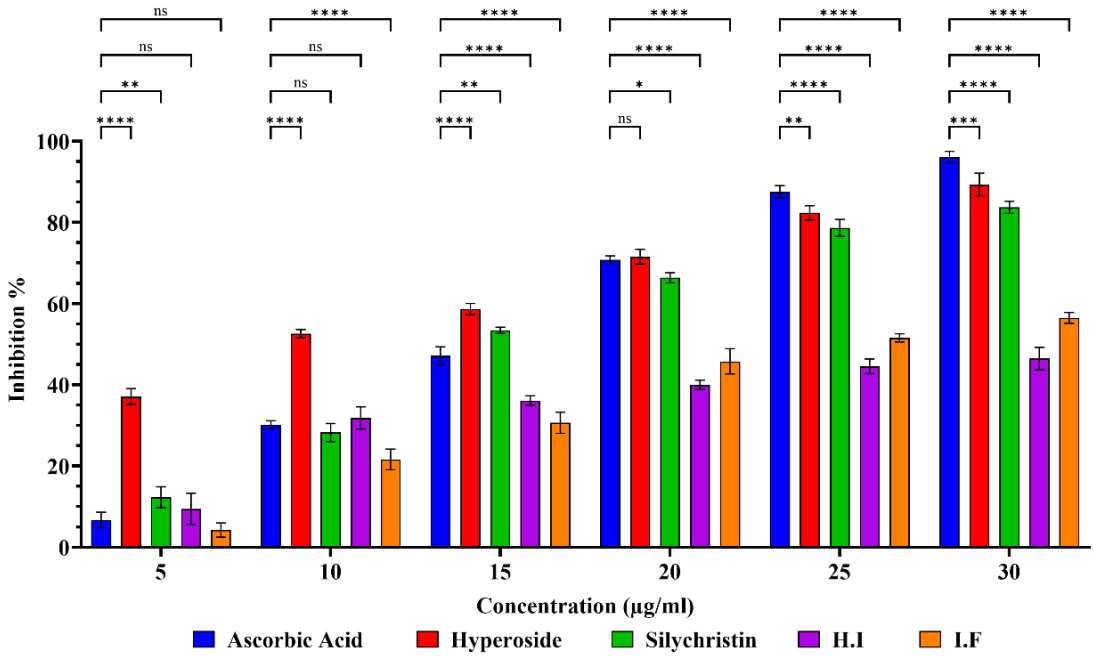

Figure 4.1: DPPH free radical scavenging activity of various concentrations (5–30 µg/mL) of Ascorbic Acid, Hyperoside, Silychristin, *Hemidesmus indicus* (H.I.), and *Ichnocarpus frutescens* (I.F.). Bars show mean ± SD; n = 3 independent replicates per concentration per treatment. Statistics were performed in GraphPad Prism using a two-way ANOVA with factors treatment × concentration, followed by Tukey's multiple-comparisons post hoc test. Brackets denote the pairwise comparisons evaluated at each concentration. Significance: $P < 0.05$ (*), $P < 0.01$ (**), $P < 0.001$ (***), $P < 0.0001$ (****); ns = not significant ($P = NS$) (two-tailed, $\alpha = 0.05$).

Hyperoside showed the most potent antioxidant compounds, with an IC_{50} value of 8.57 µg/mL, which was lowest among all. This indicated that Hyperoside was more efficient in scavenging free radicals at lower concentrations. At the highest concentrations tested (25 and 30 µg/mL), Hyperoside showed nearly 80% inhibition of DPPH radicals. Its significant activity could be attributed to its molecular structure, notably the catechol (ortho-dihydroxy) group on its B-ring, which is well known for its potent hydrogen-

donating ability (Shamsudin et al., 2022). Additionally, the glycoside moiety enhances its aqueous solubility and stabilizes the flavonoid radical formed after hydrogen donation, facilitating better radical scavenging in polar systems such as the DPPH assay. The sugar moiety also contributes to stabilization of the flavonoid's radical form after hydrogen donation, prolonging its antioxidant action (Dahiya et al., 2023). Hyperoside's strong radical scavenging capability makes it particularly effective at directly neutralizing reactive oxygen species (ROS), which are implicated in oxidative stress-related pathologies such as inflammation and cancer (Piao et al., 2008).

Silychristin demonstrated moderate antioxidant activity, with an IC_{50} value of 16.2 µg/mL, slightly higher than Ascorbic Acid but lower than the extracts (H.I. and I.F.). At higher concentrations (20–30 µg/mL), Silychristin exhibited over 70% inhibition of DPPH radicals, indicating a substantial radical scavenging capacity. The lower IC_{50} compared to the plant extracts suggested that Silychristin, a pure compound, had a more direct and potent antioxidant action, possibly due to specific structural features that facilitated free radical neutralization.

The extracts of *Hemidesmus indicus* and *Ichnocarpus frutescens* showed relatively lower antioxidant activity compared to Ascorbic Acid, Hyperoside, and Silychristin. *Hemidesmus indicus* had an IC_{50} value of 29.22 µg/mL, and *Ichnocarpus frutescens* had an IC_{50} of 24.64 µg/mL. This indicated that higher concentrations of these extracts were required to achieve a similar level of free radical scavenging as the other compounds. However, at higher concentrations (25 and 30 µg/mL), these extracts still showed significant inhibition (around 50–60%), suggesting that they possessed moderate antioxidant properties. The lower activity could be due to the presence of a mixture of phytochemicals within these extracts, where the active compounds were less concentrated

compared to the isolated phytochemicals like Hyperoside and Silychristin (Rafi et al., 2020).

Therefore, Hyperoside demonstrated the highest antioxidant activity with the lowest IC_{50} value (8.57 µg/mL), indicating its strong capacity to neutralize free radicals effectively. Ascorbic Acid also showed strong activity but with a slightly higher IC_{50} (15.75 µg/mL). Silychristin, while effective, required a higher concentration to reach 50% inhibition, as reflected in its IC_{50} value (16.2 µg/mL). The plant extracts (H.I. and I.F.) exhibited moderate activity with higher IC_{50} values, indicating less potency in free radical scavenging compared to the pure compounds. The varying antioxidant activities observed were likely due to the structural differences in these compounds, influencing their ability to donate electrons or hydrogen atoms to neutralize free radicals.

4.3.2 FRAP Assay

The Ferric Reducing Antioxidant Power (FRAP) assay evaluates the antioxidant capacity of phytochemicals and extracts by measuring their ability to reduce ferric (Fe^3+) ions to ferrous (Fe^2+) ions. In this, the inhibition percentage, which corresponds to the reduction potential, was measured across various concentrations (20–120 µg/mL) of phytochemicals, including Hyperoside, Silychristin, and methanol extract of Hemidesmus indicus (H.I.), and Ichnocarpus frutescens (I.F.) and standard drug Ascorbic Acid. The Ferric Reducing Antioxidant Power assay of different concentrations of phytochemicals, extracts of Hemidesmus indicus and Ichnocarpus frutescens, and the standard drug, Ascorbic Acid, has been illustrated in Figure 4.2. Ascorbic Acid exhibited a strong ferric-reducing ability across all tested concentrations. At the highest concentration of 120 µg/mL, it achieved nearly 90% inhibition, indicating a significant reduction of ferric ions. The IC_{50} value for Ascorbic Acid was calculated as 44.37 µg/mL,

signifying the concentration required to achieve 50% inhibition. This low IC_{50} value reflects the high antioxidant potency of Ascorbic Acid.

Silychristin demonstrated the most potent ferric-reducing ability among the tested compounds, achieving over 80% inhibition at concentrations above 80 µg/mL. Its IC_{50} value was determined to be 23.32 µg/mL, indicating a higher antioxidant capacity than Ascorbic Acid. This lower IC_{50} value suggests that Silychristin can achieve a significant antioxidant effect at a lower concentration.

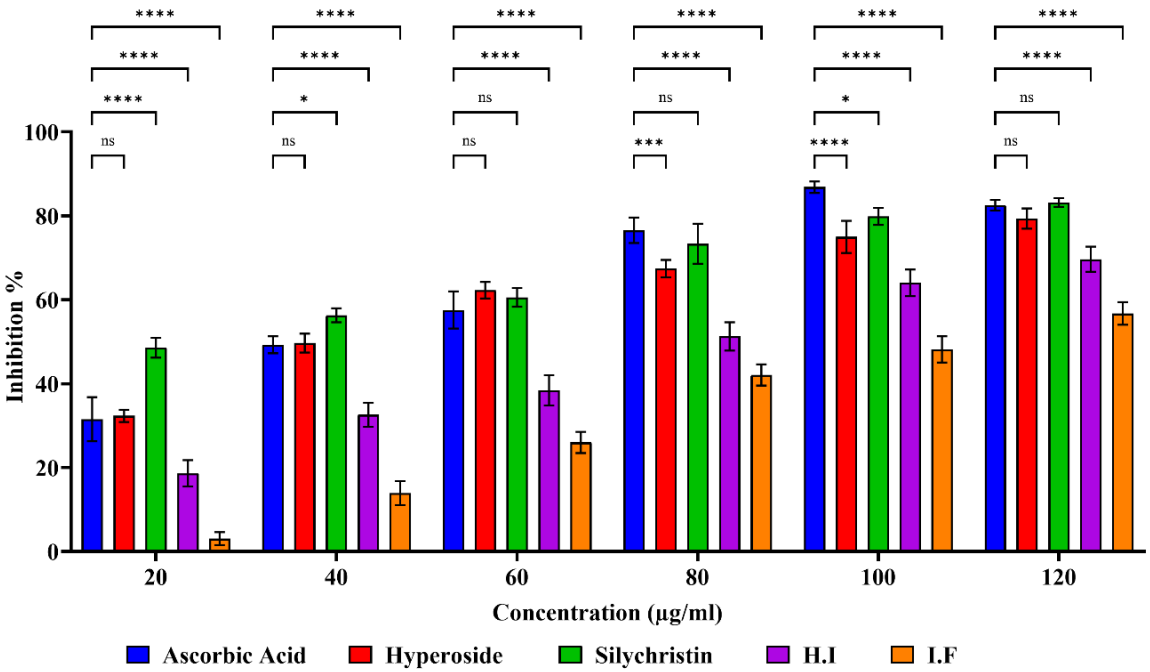

Figure 4.2: The Ferric Reducing Antioxidant Power assay of various concentrations (20–120 µg/mL) of Ascorbic Acid, Hyperoside, Silychristin, *Hemidesmus indicus* (H.I.), and *Ichnocarpus frutescens* (I.F.). Bars show mean ± SD; n = 3 independent replicates per concentration per treatment. Statistics were performed in GraphPad Prism using a two-way ANOVA with factors treatment × concentration, followed by Tukey's multiple-comparisons post hoc test. Brackets denote the pairwise comparisons evaluated at each concentration. Significance: $P < 0.05$ (*), $P < 0.01$ (**), $P < 0.001$ (***), $P < 0.0001$ (****); ns = not significant ($P = NS$) (two-tailed, $\alpha = 0.05$).

The high reduction potential observed for Silychristin can be attributed to its molecular scaffold, rich in hydroxyl groups and conjugated systems, which enables effective electron transfer and charge stabilization (AbouZid and Ahmed, 2013). Although

silychristin lacks the catechol B-ring found in hyperoside, its structure facilitates potent reducing power, making it a robust antioxidant in contexts involving electron donation and metal ion reduction. Silychristin's enhanced ferric-reducing power suggests a role in maintaining cellular redox homeostasis by preventing oxidative damage through metal ion reduction and enzyme protection (Bello, 2023).

Hyperoside showed moderate ferric reducing activity compared to Silychristin and Ascorbic Acid. It achieved an inhibition rate of approximately 70% at the highest tested concentration (120 µg/mL). The IC_{50} value for Hyperoside was 45.78 µg/mL, which is close to that of Ascorbic Acid, indicating that it has a comparable antioxidant capacity. The reduction potential of Hyperoside is likely due to the presence of multiple hydroxyl groups in its structure, which can participate in electron donation. However, its higher IC_{50} value compared to Silychristin suggests that it requires a higher concentration to exert a similar antioxidant effect.

The extracts of *Hemidesmus indicus* and *Ichnocarpus frutescens* displayed lower ferric reducing activities compared to the pure phytochemicals. *Hemidesmus indicus* exhibited an IC_{50} value of 103.38 µg/mL, while *Ichnocarpus frutescens* had an IC_{50} of 78.30 µg/mL. These higher IC_{50} values indicate that these extracts have a relatively weaker antioxidant capacity, requiring higher concentrations to achieve similar inhibition percentages. At the highest concentration (120 µg/mL), both extracts showed moderate inhibition (around 60–70%). The reduced activity can be attributed to the complex nature of the extracts, which contain a mixture of compounds, not all of which may have strong reducing abilities. The presence of active phytochemicals in lower concentrations within these extracts might lead to a less potent overall antioxidant effect compared to isolated compounds like Silychristin and Hyperoside.

Overall, the FRAP assay demonstrated that Silychristin has the highest ferric-reducing antioxidant power, as evidenced by its low IC_{50} value of 23.32 µg/mL. This suggests that it is the most effective in reducing ferric ions at lower concentrations, making it a potent antioxidant. Ascorbic Acid, while effective, showed a slightly higher IC_{50} (44.37 µg/mL), demonstrating its strong yet less efficient reducing ability compared to Silychristin. Hyperoside displayed a moderate antioxidant effect, with an IC_{50} close to Ascorbic Acid (45.78 µg/mL). In contrast, the plant extracts (H.I. and I.F.) exhibited the lowest ferric-reducing capacities, as reflected in their higher IC_{50} values, indicating that they are less effective antioxidants in the FRAP assay. The differences in antioxidant activities are likely due to variations in the molecular structures of the compounds, influencing their ability to donate electrons and reduce ferric ions.

4.3.3 Drug-Likeness and ADMET Profiling

The ADMET and toxicity profiling of hyperoside and silychristin reveal distinct characteristics that impact their potential as therapeutic agents. Table 4.1 represents the ADMET and toxicity profiles of hyperoside and silychristin. Hyperoside, with its high polarity and multiple hydroxyl groups, only partially adheres to Lipinski's Rule of Five, suggesting limitations in oral bioavailability and membrane permeability. In contrast, silychristin has a more favourable drug-likeness profile, featuring balanced lipophilicity and hydrogen bond properties, which indicate a higher likelihood of oral absorption. Hyperoside’s hydrophilic nature results in low oral bioavailability, potentially limiting its penetration through the blood-brain barrier (BBB) and leading to high plasma protein binding. Silychristin, being more lipophilic, shows better oral absorption and may cross the BBB more effectively, allowing for broader tissue distribution.

Table 4.1: ADMET and toxicity profiles of hyperoside and silychristin.

Category	Hyperoside	Silychristin
Lipinski's Rule of Five		
Molecular Weight (< 500 g/mol)	464.38 g/mol	482.44 g/mol
LogP (< 5)	0.7	2.3
Hydrogen Bond Donors (≤ 5)	8	4
Hydrogen Bond Acceptors (≤ 5)	11	8
Polar Surface Area (PSA) (< 140 Å²)	181 Å²	164 Å²
Pharmacokinetics & Dynamics		
Absorption	Low oral bioavailability due to high hydrophilicity	Higher oral absorption due to balanced lipophilicity
Membrane Permeability	Poor membrane permeability	Better membrane permeability
Blood-Brain Barrier (BBB) Penetration	Limited, due to high polarity and hydrophilicity	More likely to penetrate due to lipophilicity
Plasma Protein Binding	High binding due to hydrophilicity	Moderate binding, better tissue distribution
Metabolism	Primarily Phase II (glucuronidation, sulfation)	Undergoes both Phase I and Phase II metabolism
Excretion	Rapid renal excretion, shorter half-life	Biliary excretion, longer duration of action
Toxicity (AMES Test)	Non-mutagenic, low risk of genotoxicity, manageable skin sensitization	Non-mutagenic, low risk of genotoxicity, manageable skin sensitization
Formulation Considerations	Requires optimization to enhance bioavailability	May need formulation for optimized bioavailability

In terms of metabolism and excretion, hyperoside undergoes phase II metabolism, primarily through glucuronidation and sulfation, which leads to rapid renal excretion and a shorter half-life. This suggests a need for frequent dosing to maintain its therapeutic levels. Silychristin, on the other hand, undergoes both phase I and phase II metabolic processes, resulting in biliary excretion and potentially offering a longer duration of action due to its metabolic stability.

Toxicity assessments, including the AMES test, indicate that both hyperoside and silychristin exhibit non-mutagenic, posing a low risk of genotoxicity and manageable skin sensitization risks. Enhancing their bioavailability through formulation optimization will be key to maximizing their therapeutic potential.

4.3.4 Computational Study

4.3.4.1 Molecular Docking

The docking study between the compounds (Silychristin, Hyperoside, and Ascorbic Acid) and Xanthine Oxidase revealed significant differences in binding affinities, primarily driven by the number and nature of hydrogen bonds, pi-pi stacking interactions, and hydrophobic contacts. 2D image showing the Molecular docking interactions of Xanthine Oxidase with Silychristin, Hyperoside, and Ascorbic Acid has been depicted in Figure 4.3. Each compound interacts with specific residues in the enzyme's active site, contributing to the docking scores, which represent the strength of binding between the ligand and the enzyme.

Silychristin demonstrated the strongest binding affinity to Xanthine Oxidase, as indicated by its docking score of -9.088 kcal/mol. This strong binding can be attributed to the numerous interactions between Silychristin and key residues in the enzyme's active site. Hydrogen bonding plays a significant role in stabilizing Silychristin within the active site. Thr1010 forms a hydrogen bond with one of Silychristin's hydroxyl groups, contributing to the ligand's stabilization. Another critical hydrogen bond is formed with His875, where the nitrogen in the imidazole ring interacts with the hydroxyl group of Silychristin's flavonoid backbone, anchoring the ligand securely. Ser876 also contributes to the stabilization by forming a hydrogen bond with Silychristin's polyphenolic structure, further securing its orientation in the binding pocket. In addition to hydrogen bonds, pi-pi stacking interactions between Phe1009 and the aromatic ring of Silychristin further

stabilize the ligand. This interaction enhances the binding by locking the aromatic system of Silychristin in place, which is crucial for the ligand's affinity. Furthermore, Glu802 forms an electrostatic hydrogen bond with Silychristin, significantly adding to the overall stabilization of the ligand in the enzyme's active site. Hydrophobic interactions also play a role in stabilizing Silychristin, with residues such as Leu873, Val1011, and Phe1013 interacting with the non-polar regions of the ligand, contributing to its strong binding. The combination of multiple hydrogen bonds, pi-pi stacking, and hydrophobic interactions explains why Silychristin has the lowest docking score and the highest inhibition potential against Xanthine Oxidase.

Hyperoside exhibited a strong binding affinity for Xanthine Oxidase, with a docking score of -7.270 kcal/mol, although it was slightly weaker than Silychristin. Similar to Silychristin, Hyperoside's binding is mediated by multiple hydrogen bonds and pi-pi stacking interactions. Thr1010 forms a hydrogen bond with Hyperoside, stabilizing the ligand in the enzyme's active site. His875 also contributes a hydrogen bond, interacting with Hyperoside's sugar-like structure, which helps anchor the ligand. Another critical residue, Asp872, forms a strong hydrogen bond with Hyperoside, providing additional electrostatic stabilization. These hydrogen bonds are vital for maintaining Hyperoside's orientation and binding within the enzyme. The role of Phe914 is significant in Hyperoside's binding. This residue not only forms a hydrogen bond but also participates in pi-pi stacking with the planar aromatic ring of Hyperoside, further stabilizing the ligand through aromatic interactions. Hydrophobic residues such as Leu873, Pro1076, and Val1011 interact with the non-polar regions of Hyperoside, providing additional stabilization to the ligand within the hydrophobic pocket of Xanthine Oxidase. However, despite these strong interactions, Hyperoside's docking score is slightly higher than

Silychristin's, likely due to fewer pi-pi stacking interactions and a less extensive network of hydrogen bonds.

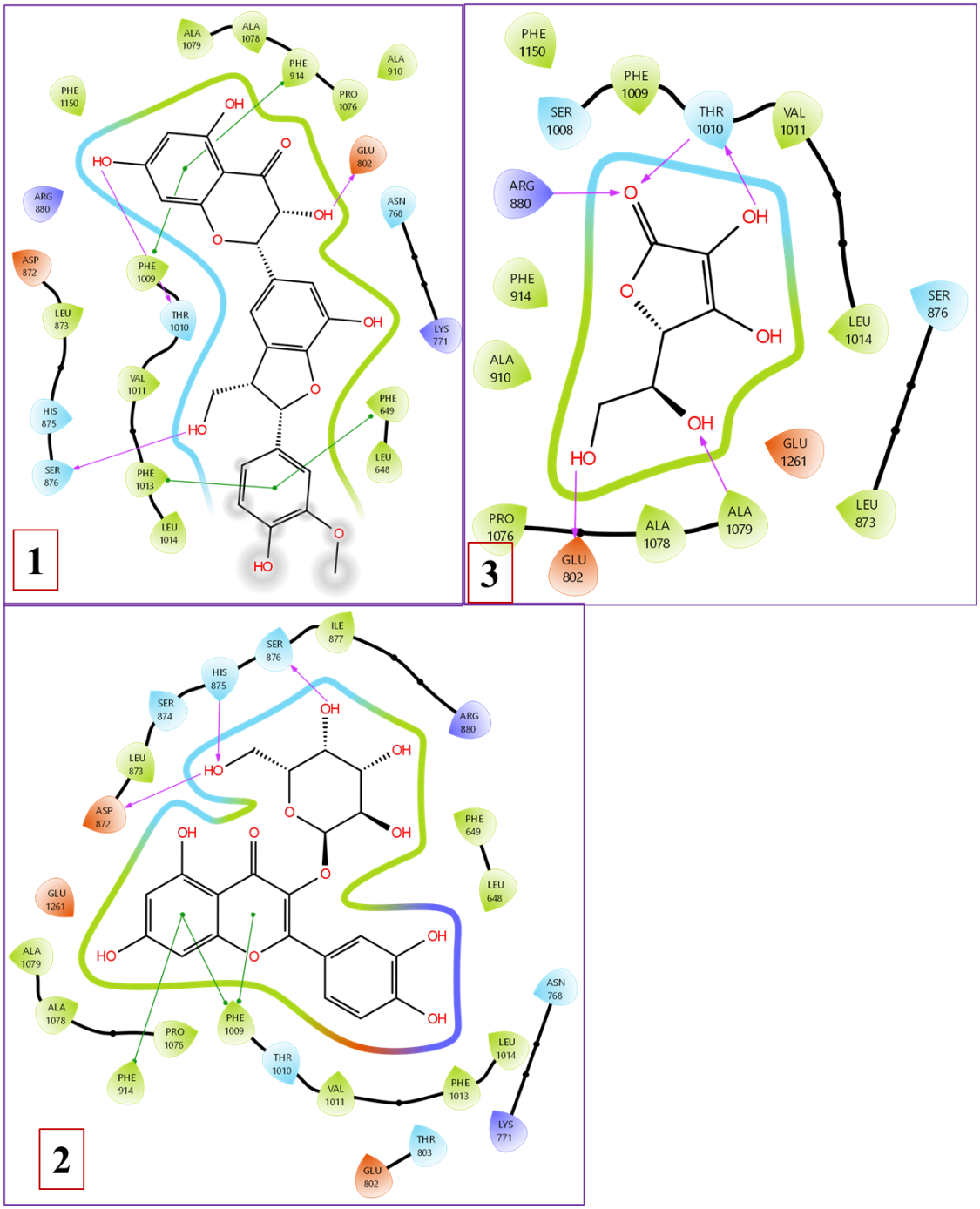

Figure 4.3: 2D image showing the Molecular docking interactions of Xanthine Oxidase with Silychristin (1), Hyperoside (2), and Ascorbic Acid (3).

Ascorbic Acid exhibited the weakest binding affinity to Xanthine Oxidase, with a docking score of -5.086 kcal/mol. Although it forms some important hydrogen bonds, the overall

interaction profile of Ascorbic Acid is less robust compared to Silychristin and Hyperoside. Glu802 plays a central role in stabilizing Ascorbic Acid by forming a hydrogen bond with the ligand's hydroxyl group. This interaction contributes to the electrostatic stabilization of Ascorbic Acid within the enzyme's binding site. Pro1076 and Ala1079 also form hydrogen bonds with Ascorbic Acid, further stabilizing the ligand by interacting with its carboxyl and hydroxyl groups. While Ascorbic Acid benefits from these hydrogen bonds, it lacks the extensive pi-pi stacking interactions observed in the other two ligands, which limits its overall binding affinity. Moreover, the hydrophobic interactions formed by residues such as Leu873 and Ser876 are relatively weak and fewer in number, offering only limited support for ligand stabilization. The absence of strong pi-pi stacking and a reduced number of hydrogen bonds contribute to the higher docking score of Ascorbic Acid, making it the least potent inhibitor of Xanthine Oxidase compared to Hyperoside and Silychristin

Thus, overall docking results demonstrated that Silychristin exhibits the strongest binding affinity (-9.088 kcal/mol) due to its extensive network of hydrogen bonds (with Thr1010, His875, Ser876, and Glu802), along with pi-pi stacking with Phe1009 and hydrophobic interactions. Hyperoside also forms strong hydrogen bonds with Thr1010, His875, Asp872, and Phe914, and benefits from pi-pi stacking with Phe914, resulting in a slightly weaker binding affinity (-7.270 kcal/mol). Ascorbic Acid, with fewer hydrogen bonds and weaker hydrophobic interactions, exhibits the weakest binding affinity (-5.086 kcal/mol). The lack of pi-pi stacking and a less extensive hydrogen bonding network make Ascorbic Acid a less effective inhibitor of Xanthine Oxidase compared to the other two ligands.

4.3.4.2 Molecular Dynamic Simulation

Molecular dynamics (MD) simulations were carried out on a 100 ns using the Schrödinger Maestro tool in order to verify the docking results. These simulations aimed to study the

dynamic interactions and stability of the Xanthine oxidase enzyme when complexed with ligands Hyperoside, Silychristin, and standard drug Ascorbic Acid. Docking initially provided a static snapshot of the interactions between Xanthine oxidase and the ligands. However, docking alone cannot capture the dynamic nature of protein-ligand interactions in a physiological environment, where both the protein and ligand are in constant motion. Therefore, MD simulations were conducted to offer a more realistic and detailed understanding of these interactions over time, allowing for the assessment of how each ligand affects the enzyme's structure and stability under near-physiological conditions. During the 100 ns MD simulations, several key parameters were monitored to evaluate the stability and conformational changes of the Xanthine oxidase -ligand complexes. These included the root-mean-square deviation (RMSD), root-mean-square fluctuation (RMSF) radius of gyration (RoG), Solvent Accessible Surface Area (SASA) and the number of hydrogen bonds. This comprehensive MD analysis helped to identify the ligand that forms the most stable and effective inhibitory complex with Xanthine oxidase. Figure 4.4 depicted the Root Mean Square Deviation profile of Xanthine Oxidase in its apo state and when complexed with Hyperoside, Silychristin, and the standard drug Ascorbic Acid over the 100 ns MD. The RMSD plot demonstrated the conformational stability of Xanthine Oxidase (XO) in its apo form and when complexed with Hyperoside, Silychristin, and Ascorbic Acid.

For the apo form, the RMSD stabilized around 1.5–2 Å, indicating a stable structure in the absence of ligands. Upon ligand binding, there were initial increases in RMSD within the first 10 ns, reflecting structural adjustments as the protein accommodated the ligands. Hyperoside exhibited RMSD fluctuations between 1.5 and 2.5 Å after this initial period, indicating that it induced flexibility within the protein structure.

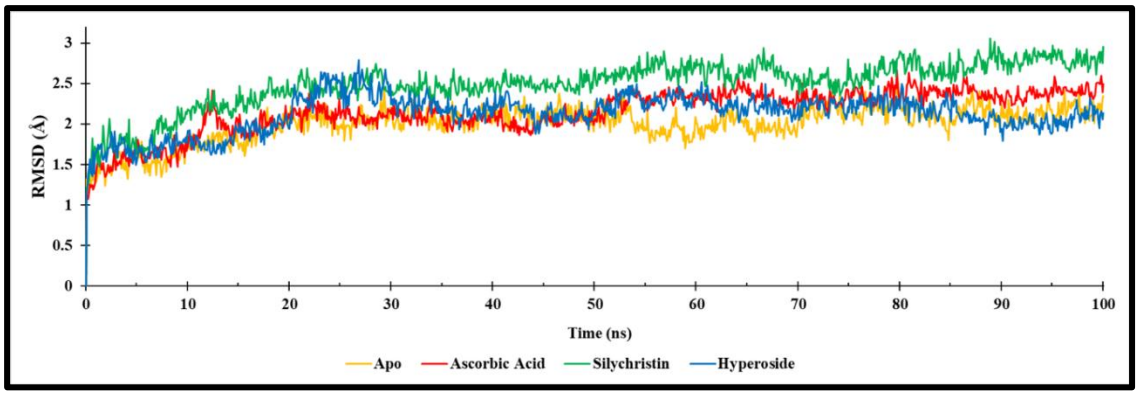

Figure 4.4: Root Mean Square Deviation profile of Xanthine Oxidase in its apo state (yellow) and complexed with ligands Hyperoside (blue), Silychristin (green), and Ascorbic Acid (red) over the 100 ns Molecular Dynamics simulation.

This flexibility involved the rearrangement of active site residues, including those critical for catalytic activity, such as Glu1261 and Arg880, which slightly shifted to optimize binding. While Hyperoside fit well into the binding pocket, it also induced a degree of conformational freedom, altering the enzyme's active site in a manner that could affect its catalytic function. Silychristin showed a more stable RMSD profile, averaging around 1.5–2 Å after stabilization, suggesting that it bound in a manner that caused minimal perturbation to the protein's overall structure. This binding involved anchoring interactions with key residues, such as hydrogen bonding with Thr1010 or Glu802, resulting in a more rigid and stable complex. Ascorbic Acid, despite its smaller size, maintained a consistent RMSD similar to that of Silychristin, indicating that it also bound without inducing significant conformational changes. Its interaction involved surface-level binding or the occupation of a shallow pocket, stabilizing the protein through weaker yet consistent interactions. The stability across these RMSD profiles indicated that all three ligands maintained the structural integrity of XO, with Hyperoside inducing the most flexibility, suggesting a different mode of interaction compared to Silychristin and Ascorbic Acid. Figure 4.5 depicted the Solvent Accessible Surface Area of Xanthine Oxidase when complexed with Hyperoside, Silychristin, and the standard drug Ascorbic Acid. The SASA values provided insights into how each ligand modulated XO's structural

conformation by showing the extent of the protein's surface exposed to the solvent (Agarwal et al., 2022).

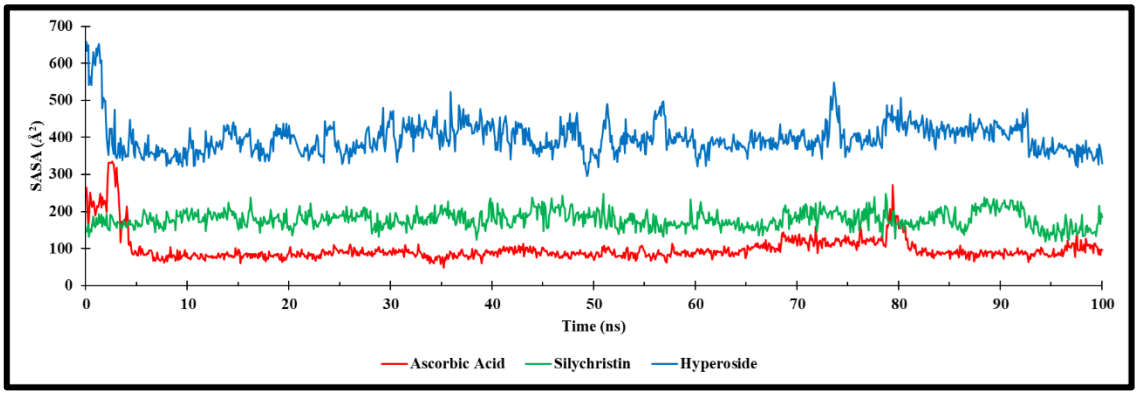

Figure 4.5: Solvent Accessible Surface Area of Xanthine Oxidase when complexed with ligands Hyperoside (blue), Silychristin (green), and Ascorbic Acid (red) over the 100 ns Molecular Dynamics simulation.

Hyperoside binding resulted in a significant increase in SASA, stabilizing between 500–600 Å². This suggested that Hyperoside induced a conformational change that exposed more surface area to the solvent, possibly through the opening of the active site or movement of surface loops. This conformational change involved the displacement of flexible regions or loops surrounding the active site, allowing Hyperoside to interact deeply with residues that were typically buried, such as Phe914 or Leu873. The exposure of these internal residues to the solvent enhanced the ligand's binding interactions, facilitating access to key catalytic residues and potentially altering the enzyme's activity. Silychristin displayed a moderate increase in SASA, around 300–400 Å², indicating a partial opening of the protein structure. This partial opening suggested that Silychristin bound within the active site and induced some degree of conformational change, but not to the same extent as Hyperoside. Its binding involved interactions that stabilized certain regions of the protein, including hydrogen bonds with surface residues like Thr1010 or hydrophobic interactions with nearby nonpolar residues, without causing extensive reorganization of the protein's tertiary structure. Ascorbic Acid-bound XO maintained a

low SASA, indicating the preservation of the protein's compact conformation. Ascorbic Acid interacted with surface-accessible residues or shallow pockets without penetrating deeply into the active site. This minimal impact on the protein's surface exposure implied that Ascorbic Acid did not induce significant conformational changes, largely due to its smaller size and limited functional groups necessary for disrupting the protein's structure.

Figure 4.6 depicted the Radius of Gyration profile of Xanthine Oxidase when complexed with Hyperoside, Silychristin, and the standard drug Ascorbic Acid. The RoG measured the distribution of the protein's mass around its center, indicating how compact or extended the protein was during the simulation.

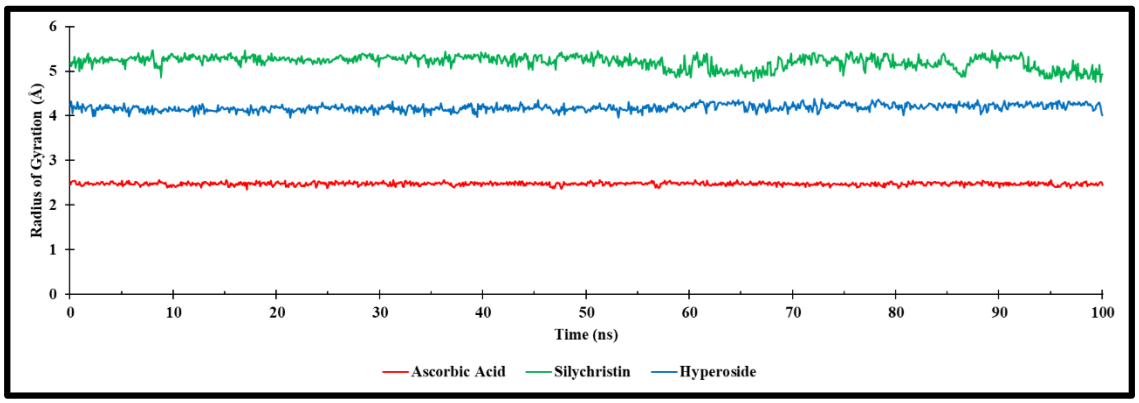

Figure 4.6: Radius of Gyration profile of Xanthine Oxidase when complexed with ligands Hyperoside (blue), Silychristin (green), and Ascorbic Acid (red) over the 100 ns Molecular Dynamics simulation.

When XO bound to Ascorbic Acid, the RoG remained consistent around 5 Å, indicating a stable and compact protein conformation. This consistency suggested that the protein's core remained tightly packed with little to no expansion of its tertiary structure. The minimal changes in RoG for Ascorbic Acid indicated that this ligand did not cause significant global structural rearrangements, likely because of its binding in a manner that did not disturb the overall protein conformation. Hyperoside, on the other hand, exhibited a slightly higher RoG, around 5.5 Å, indicating a more expanded protein structure. This expansion correlated with the higher SASA values observed, showing that Hyperoside

binding induced conformational changes that increased the protein's overall size. Hyperoside interacted with residues that were normally part of the protein's core, resulting in a rearrangement that led to a more relaxed, open structure. This interaction involved residues that modulated the accessibility of the active site, enhancing binding affinity while allowing for a flexible fit within the binding pocket. Silychristin displayed an intermediate RoG around 5.25 Å, suggesting moderate expansion. Silychristin induced some conformational adjustments, potentially stabilizing specific regions like surface loops or secondary structural elements near the binding site. This led to a modest increase in the protein's overall size without destabilizing the structure.

Figure 4.7 depicts the Number of Hydrogen Bonds profile of Xanthine Oxidase when complexed with Hyperoside, Silychristin, and the standard drug Ascorbic Acid. The number of hydrogen bonds was crucial for understanding the interaction strength and stability between XO and the ligands.

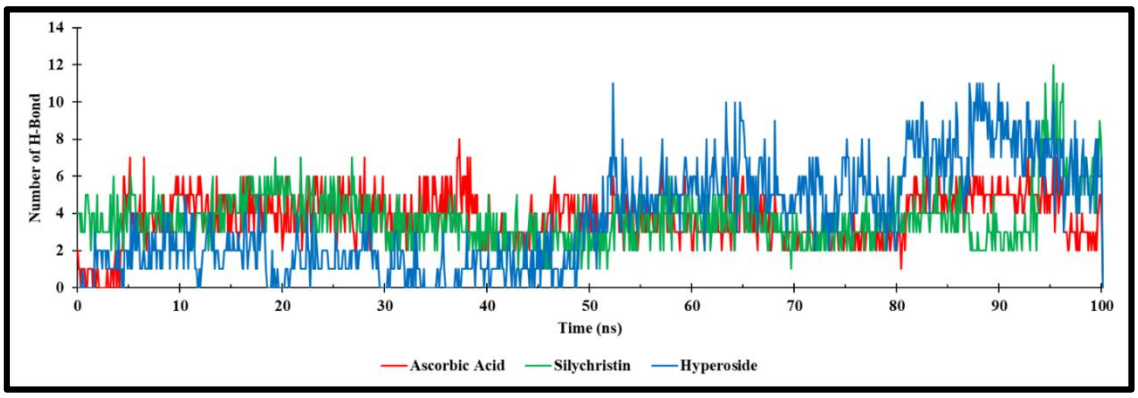

Figure 4.7: Number of Hydrogen Bonds profile of Xanthine Oxidase when complexed with ligands Hyperoside (blue), Silychristin (green), and Ascorbic Acid (red) over the 100 ns Molecular Dynamics simulation.

Hyperoside formed the highest number of hydrogen bonds, fluctuating between 5 and 10 throughout the simulation. Hyperoside established a robust and dynamic hydrogen-bonding network with key active site residues such as Glu1261, Arg880, and Phe914. The frequent formation and maintenance of these hydrogen bonds indicated strong and

persistent interactions that contributed to the stability of the Hyperoside-XO complex. These interactions involved both the backbone and side chains of residues, stabilizing the enzyme in a specific conformation that potentially inhibited its catalytic activity by blocking substrate access or altering the active site's geometry. Silychristin formed a moderate number of hydrogen bonds, ranging between 3 and 7, indicating stable binding involving specific interactions with residues such as Thr1010 or Glu802. Although the number of hydrogen bonds was lower than that of Hyperoside, Silychristin compensated by forming strong hydrophobic interactions with surrounding residues, contributing to the stability of the complex. The binding of Silychristin involved anchoring interactions that maintained the protein's overall conformation while subtly modulating the active site's dynamics. Ascorbic Acid formed the fewest hydrogen bonds, typically fluctuating between 1 and 4, indicating weaker interactions with XO. This was attributed to Ascorbic Acid's smaller size and fewer functional groups capable of forming hydrogen bonds. Its binding relied on van der Waals contacts and weaker polar interactions, resulting in a less stable complex. The low number of hydrogen bonds formed by Ascorbic Acid indicated that it did not effectively occupy the active site or influence the enzyme's activity to the same extent as the other ligands.

Figure 4.8 displayed the Root Mean Square Fluctuation plot showing the flexibility and dynamic behaviour of individual residues within Xanthine Oxidase (XO) during the molecular dynamics simulation of 100 ns (Singh and Mishra, 2020). RMSF is a critical measure for understanding the local flexibility of protein regions, which can influence the binding dynamics and catalytic efficiency of enzymes. Residues with high RMSF values indicate regions of the protein that experience significant fluctuations, which can be associated with loops, active site flexibility, or conformational changes upon ligand binding.

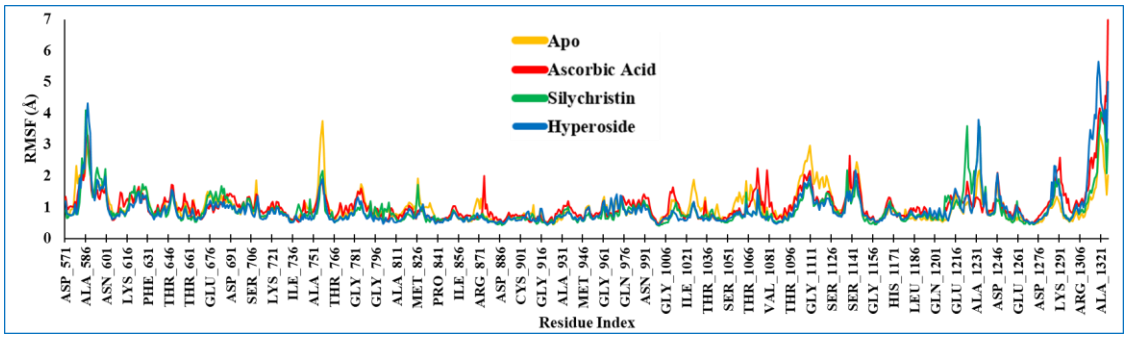

Figure 4.8: Root Mean Square Fluctuation (RMSF) profiles of Xanthine Oxidase in its apo form and in complex with Ascorbic Acid, Silychristin, and Hyperoside.

In the apo state, significant fluctuations were observed in regions such as Asp571, Ala586, and Lys731, with RMSF values peaking around 3–4 Å. These regions likely correspond to flexible loops or surface-exposed areas, contributing to the enzyme's intrinsic flexibility in the absence of any bound ligand. The observed flexibility in these regions could be essential for accommodating substrate binding and facilitating enzymatic activity. Additionally, higher RMSF values in the terminal regions suggest typical end-region flexibility, a common characteristic in proteins where the termini are less structurally constrained. Notably, residues near the active site, such as Glu1261 and Arg880, exhibited lower RMSF values, indicating that the core active site region maintains its structural integrity, which is crucial for catalytic function.

When Xanthine Oxidase was complexed with Ascorbic Acid, the RMSF profile closely resembled the apo state, suggesting that Ascorbic Acid binding did not significantly alter the flexibility of the protein. However, there were slight reductions in fluctuation around residues like Thr909 and Thr1010, indicating that Ascorbic Acid might have interacted with these regions to provide marginal stabilization. Due to the small size and limited interaction surface of Ascorbic Acid, its binding likely involved surface-level interactions that did not penetrate deeply into the protein structure. This lack of deep binding led to a minimal influence on the protein's overall dynamics, explaining the subtle differences in RMSF compared to the apo form.

Silychristin binding resulted in a noticeable reduction in the fluctuation of certain residues, particularly around the active site region, including residues like Glu802 and Thr1010, which exhibited reduced RMSF values compared to the apo form and the Ascorbic Acid complex. This reduction in flexibility suggests that Silychristin interacted strongly with key residues in the active site, forming stable hydrogen bonds or hydrophobic interactions. For instance, Silychristin may have formed hydrogen bonds with residues such as Glu802 or Thr1010, anchoring itself within the active site and thereby restricting the movement of surrounding residues. Moreover, the binding of Silychristin may have led to a more rigid conformation of surface loops, which is indicative of a more stable and possibly inhibitory protein-ligand complex, preventing substrate access and hence modulating enzymatic activity.

Hyperoside binding induced the most significant changes in the RMSF profile, particularly in regions around residues Lys731, Thr1010, and Glu1261. RMSF values in these regions were reduced, indicating that Hyperoside binding led to the stabilization of both surface-exposed loops and the active site. This stabilization likely involved multiple interactions, such as hydrogen bonding with Glu1261 and Arg880, as well as hydrophobic contacts with residues like Phe914. These interactions would result in a more rigid conformation around the active site, potentially blocking substrate access or altering the enzyme's catalytic machinery. The reduced fluctuations in regions such as Thr1010 and Glu1261 suggest that Hyperoside effectively anchored itself within the active site, inducing a structural rigidity that could inhibit enzyme function. The decrease in flexibility in these regions implies that Hyperoside may have enforced a conformational state of the enzyme that is less favourable for catalysis, thus showcasing its potential as a strong inhibitor.

Overall, the RMSF analysis shows that Hyperoside and Silychristin significantly stabilize Xanthine Oxidase more than Ascorbic Acid. Hyperoside had the strongest effect, especially at the active site, reducing the mobility of key residues and likely inhibiting enzyme activity. Silychristin also restricted movement, though less than Hyperoside, indicating effective binding. In contrast, Ascorbic Acid showed minimal impact, suggesting weaker, surface-level interactions. Overall, hyperoside and silychristin are more capable of modulating the enzyme's dynamics than ascorbic acid.

4.3.4.3 MMGBSA analysis

MMGBSA analysis of the binding interactions between Xanthine Oxidase and the ligands Silychristin, Ascorbic Acid, and Hyperoside, detailing various energy components over the last 20% of the total simulation frames in kcal/mol is represented in Table 4.2. Silychristin exhibited the most negative binding free energy (ΔGbind = -56.93 kcal/mol), indicating the strongest binding affinity to Xanthine Oxidase among the three ligands. This high binding energy was primarily due to a significant Coulombic contribution (ΔEcoulomb = -31.57 kcal/mol), suggesting strong electrostatic interactions between Silychristin and charged or polar residues within the binding site. Such interactions often involve hydrogen bonding and ionic contacts, which can lead to specific and tight binding. The Van der Waals energy (ΔEvdW = -47.59 kcal/mol) also contributed substantially to the binding, indicating that Silychristin effectively occupied the hydrophobic regions of the binding pocket. This suggests extensive hydrophobic interactions and close van der Waals contacts with nonpolar residues, which stabilize the complex. Additionally, the lipophilic energy (ΔElipo = -18.62 kcal/mol) implies that Silychristin interacted favourably with lipophilic pockets within the enzyme, likely involving interactions with aromatic residues or hydrophobic pockets, further anchoring the ligand within the active site. The strong binding of Silychristin results from it fitting snugly into the binding

pocket, forming a network of interactions that collectively enhance the stability of the enzyme-ligand complex.

Table 4.2: MMGBSA profile analysis of the binding interactions between Xanthine Oxidase and the ligands Silychristin, Ascorbic Acid, and Hyperoside

MMGBSA (kcal/mol)						
Sr. No.	**Compound**	**ΔG_{bind}**	**$\Delta E_{Coulomb}$**	**ΔE_{Lipo}**	**E_{Ele}**	**ΔE_{vdW}**
1	Silychristin	-56.93	-31.57	-18.62	41.16	-47.59
2	Ascorbic Acid	-34.85	-34.07	-4.12	22.03	-17.09
3	Hyperoside	-11.04	-10.70	-2.36	14.21	-11.66

Binding free energy (ΔGbind), Coulomb energy (ΔEcoulomb), Lipophilic energy (ΔElipo), Generalized Born electrostatic solvation energy (EEle), and Van der Waals energy (ΔEvdW)

Ascorbic Acid displayed a binding free energy (ΔGbind = -34.85 kcal/mol), which, while significant, was lower than that of Silychristin. The Coulomb energy (ΔEcoulomb = -34.07 kcal/mol) contributed the most to the binding, indicating that electrostatic interactions played a crucial role in the binding process. Given Ascorbic Acid's polar nature, these interactions likely involve hydrogen bonds with key residues in the enzyme's active site, potentially with charged residues like Glu or Asp. The lower van der Waals energy (ΔEvdW = -17.09 kcal/mol) indicates that Ascorbic Acid might not occupy the binding pocket as deeply or extensively as Silychristin, potentially leading to a less stable hydrophobic environment. The lipophilic energy (ΔElipo = -4.12 kcal/mol) was also considerably lower, implying limited interactions with the enzyme's hydrophobic surfaces. This suggests that Ascorbic Acid's binding mode was more surface-oriented or involved fewer nonpolar contacts, reflecting its smaller and more polar structure.

Hyperoside showed the least negative binding free energy (ΔGbind = -11.04 kcal/mol) among the three ligands, indicating a comparatively weaker binding affinity. The Coulomb energy (ΔEcoulomb = -10.70 kcal/mol) was the primary contributor, suggesting the presence of some electrostatic interactions, though not as extensive or strong as those

seen with Silychristin or Ascorbic Acid. This could involve fewer or weaker hydrogen bonds with the enzyme's polar residues, reflecting a less optimal alignment within the active site. The Van der Waals energy (ΔEvdW = -11.66 kcal/mol) indicated moderate interactions with the enzyme's hydrophobic regions, but these were less substantial compared to the other ligands. The lipophilic energy (ΔElipo = -2.36 kcal/mol) was also the lowest, suggesting minimal interactions with nonpolar residues. This low lipophilic contribution implies that Hyperoside did not engage deeply with the hydrophobic pockets of Xanthine Oxidase, possibly occupying a more solvent-exposed binding mode or having less contact with aromatic and hydrophobic residues. The less favourable binding energetics of Hyperoside suggest that its interaction with Xanthine Oxidase was relatively weaker, possibly due to suboptimal positioning within the active site that limited its ability to form extensive stabilizing interactions.

Overall, the MMGBSA analysis shows that Silychristin demonstrated much more stable binding with Xanthine Oxidase compared to Ascorbic Acid due to its strong Coulombic and van der Waals interactions, indicating deep engagement within the binding pocket. While Ascorbic Acid showed significant electrostatic interactions, its weaker van der Waals and lipophilic contributions suggest less comprehensive binding. In contrast, Hyperoside exhibited the weakest binding overall, with minimal contributions from both electrostatic and hydrophobic interactions, pointing to a more superficial or loosely bound interaction compared to the more robust engagement seen with Silychristin and even Ascorbic Acid.

4.3.4.4 Per Residue Decomposition

The per-residue decomposition analysis depicted in Figure 4.9 provides detailed insights into the binding contributions of individual amino acid residues in Xanthine Oxidase (XO) with the ligands Ascorbic Acid, Silychristin, and Hyperoside. This analysis breaks

down the total binding free energy (ΔG_{bind}) to identify which residues contribute significantly to the stabilization or destabilization of the protein-ligand complex.

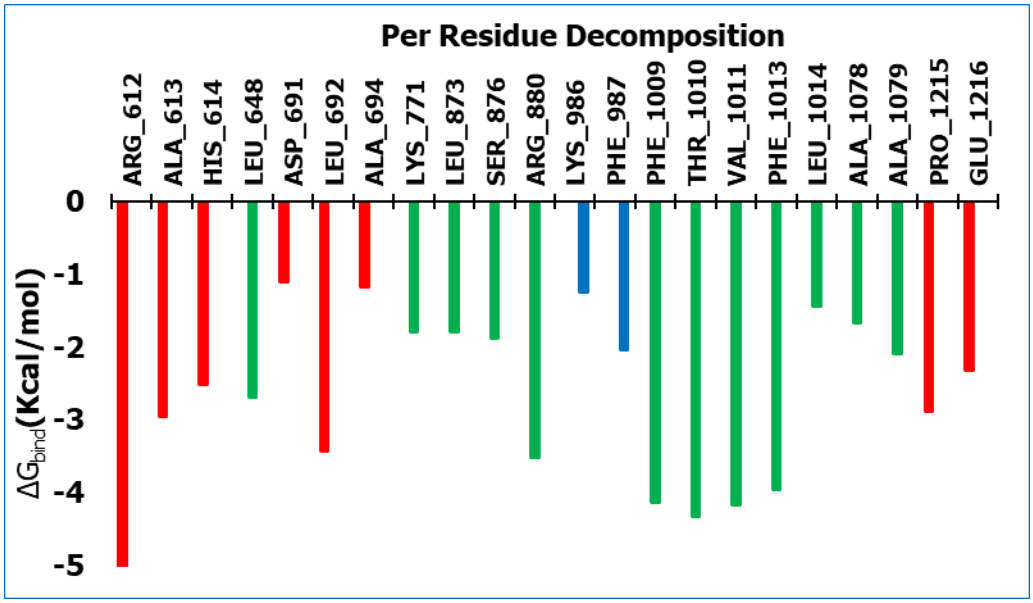

Figure 4.9: Per residue decomposition of Xanthine Oxidase showing binding contributions of individual amino acid residues with the ligands Ascorbic Acid (red), Silychristin (green) and Hyperoside (blue).

Ascorbic Acid showed favorable interactions primarily with residues Arg 612, His 614, and Asp 696, contributing significantly to the binding free energy. The binding free energy (ΔGbind) for Arg 612 and Asp 696 was highly negative, indicating strong electrostatic and hydrogen-bonding interactions. For instance, Arg 612 demonstrated a ΔG_{bind} contribution of around -3 kcal/mol, likely due to its positive charge interacting with the polar hydroxyl groups of Ascorbic Acid. Asp 696 contributed about -2 kcal/mol, suggesting a strong ionic interaction between its negatively charged side chain and the ligand. HIS 614 also contributed significantly to the binding, with a ΔG_{bind} of approximately -2.5 kcal/mol, reflecting stable hydrogen bonds formed with the ligand. These interactions indicate that Ascorbic Acid formed a stable complex with XO, mainly through polar and charged residues, but the overall ΔG_{bind} values were less negative than those observed for Silychristin, suggesting a moderate level of stabilization within the active site.

Silychristin exhibited the most substantial binding effect, with deeply penetrating interactions with key residues such as Arg 880, Phe 1009, and Thr 1010. Arg 880 showed a highly negative ΔG_{bind} contribution of around -5 kcal/mol, indicating strong electrostatic interactions with the ligand's functional groups. This suggests that Arg 880 played a crucial role in anchoring Silychristin within the binding pocket. Phe 1009 exhibited a significant ΔG_{bind} of around -4 kcal/mol, highlighting hydrophobic and π-π stacking interactions between the aromatic rings of Silychristin and the phenyl side chain of Phe 1009. Thr 1010 contributed about -3 kcal/mol to the binding free energy, indicating hydrogen bonding that further stabilized the complex. Glu 1216 also contributed notably with a ΔG_{bind} of around -2.5 kcal/mol, likely involving ionic interactions. This extensive network of interactions, reflected in the highly negative per-residue ΔG_{bind} values, suggests that Silychristin forms a deeply embedded and stable complex with XO, engaging with a wide range of residues both within the active site and in surrounding regions.

Hyperoside displayed moderate interactions, as indicated by the per-residue ΔG_{bind} values. Asp 696 and Arg 880 were notable contributors to Hyperoside's binding affinity. Asp 696 contributed a ΔG_{bind} of around -2.5 kcal/mol, indicative of hydrogen bonding between its carboxyl group and the hydroxyl groups of Hyperoside. Arg 880 showed a contribution of around -2 kcal/mol, suggesting ionic or hydrogen bond interactions with the ligand. However, the overall contributions of Lys 771 and Ser 876 were less negative, around -1 to -1.5 kcal/mol, indicating weaker hydrogen bonds and electrostatic interactions compared to those formed by Silychristin. The more moderate per-residue ΔG_{bind} values for Hyperoside suggest that while it does form stabilizing interactions with several residues, its engagement with the binding pocket is not as deep or as energetically

favourable as that of Silychristin. The interactions appeared to be more surface-level, which is consistent with Hyperoside's overall weaker binding affinity.

Thus, overall analysis showed that Silychristin exhibited the most potent binding affinity, as indicated by the most negative per-residue ΔG_{bind} values. For instance, Arg 880 and Phe 1009 in the Silychristin complex showed ΔG_{bind} values around -5 kcal/mol and -4 kcal/mol, respectively, highlighting the strong electrostatic and hydrophobic interactions contributing to a highly stable protein-ligand complex. In contrast, Ascorbic Acid, while showing some strong interactions, especially with Arg612 ($\Delta G_{bind} \approx -3$ kcal/mol) and His 614 ($\Delta G_{bind} \approx -2.5$ kcal/mol), demonstrated a less negative overall binding energy, indicating less extensive penetration into the binding site. Hyperoside, with even weaker per-residue ΔGbind values such as Asp 696 ($\Delta G_{bind} \approx -2.5$ kcal/mol) and Arg 880 ($\Delta G_{bind} \approx -2$ kcal/mol), suggests that its interaction with the enzyme is more superficial, lacking the deep and energetically favorable interactions seen with Silychristin.

4.4 Conclusion

The present chapter explored the antioxidant potential of Hyperoside, Silychristin, and crude extracts of *Hemidesmus indicus* and *Ichnocarpus frutescens* through *invitro* assays, including DPPH and FRAP, along with computational analysis of their interactions with Xanthine Oxidase. The DPPH assay demonstrated that Hyperoside exhibited the most potent free radical scavenging activity, with the lowest IC_{50} (8.57 µg/mL), indicating its strong antioxidant potential due to its effective hydrogen-donating ability. Silychristin showed moderate antioxidant activity with an IC_{50} of 16.2 µg/mL, while the methanolic extracts of both plants exhibited lower activities, likely due to the presence of a mixture of phytochemicals. Ascorbic Acid, a standard antioxidant, also showed significant activity but required a higher concentration than Hyperoside. In the FRAP assay, Silychristin demonstrated the most potent ferric reducing capacity with an IC_{50} value of 23.32 µg/mL,

surpassing Ascorbic Acid and Hyperoside, reflecting its superior electron-donating ability in reducing ferric ions. The extracts showed weaker ferric-reducing capacity, aligning with their higher IC_{50} values, indicating that pure compounds like Silychristin and Hyperoside have more direct and potent antioxidant actions than complex plant extracts. Molecular docking and dynamic simulations revealed that Silychristin had the strongest binding affinity to Xanthine Oxidase (-9.088 kcal/mol), primarily due to its extensive hydrogen bonding and hydrophobic interactions with key active site residues. Hyperoside also showed strong binding affinity but was slightly weaker (-7.270 kcal/mol) compared to Silychristin, likely due to fewer pi-pi stacking interactions. Ascorbic Acid exhibited the weakest binding affinity (-5.086 kcal/mol), lacking the extensive hydrogen bond network and pi-pi stacking observed in the other compounds. The molecular dynamic simulations confirmed that Silychristin formed the most stable and rigid complex with Xanthine Oxidase, maintaining structural integrity and showing the least flexibility. Hyperoside induced more flexibility, suggesting a different mode of interaction, while Ascorbic Acid formed a less stable and weaker complex. The MMGBSA analysis supported these findings, with Silychristin demonstrating the most negative binding free energy (-56.93 kcal/mol), indicating the strongest binding, followed by Ascorbic Acid (-34.85 kcal/mol) and Hyperoside (-11.04 kcal/mol). Overall, Hyperoside and Silychristin emerged as potent antioxidants with strong free radical scavenging and ferric reducing capacities, as well as strong inhibitory potential against Xanthine Oxidase. The computational analysis confirmed their binding affinity and stability, with Silychristin showing the most potent inhibition of Xanthine Oxidase.

The findings from this chapter lay a crucial foundation for exploring the antidiabetic and anticancer potential of Hyperoside and Silychristin in the subsequent chapter. Oxidative stress not only contributes to the initiation and progression of cancer but also plays a

significant role in the pathogenesis of diabetes by impairing insulin signalling and beta-cell function. The strong antioxidant properties of these compounds suggest they may mitigate oxidative damage, thereby improving cellular function and survival. The next chapter will delve into the biological evaluation and computational studies of these compounds for their antidiabetic and anticancer activities. It will explore how their antioxidant properties translate into therapeutic effects, examining mechanisms such as enzyme inhibition, cell cycle arrest, and modulation of signalling pathways. This integrated approach aims to provide a comprehensive understanding of how Hyperoside and Silychristin can be harnessed for the prevention and treatment of diabetes and cancer, potentially leading to the development of novel therapeutic agents derived from *Hemidesmus indicus* and *Ichnocarpus frutescens*.